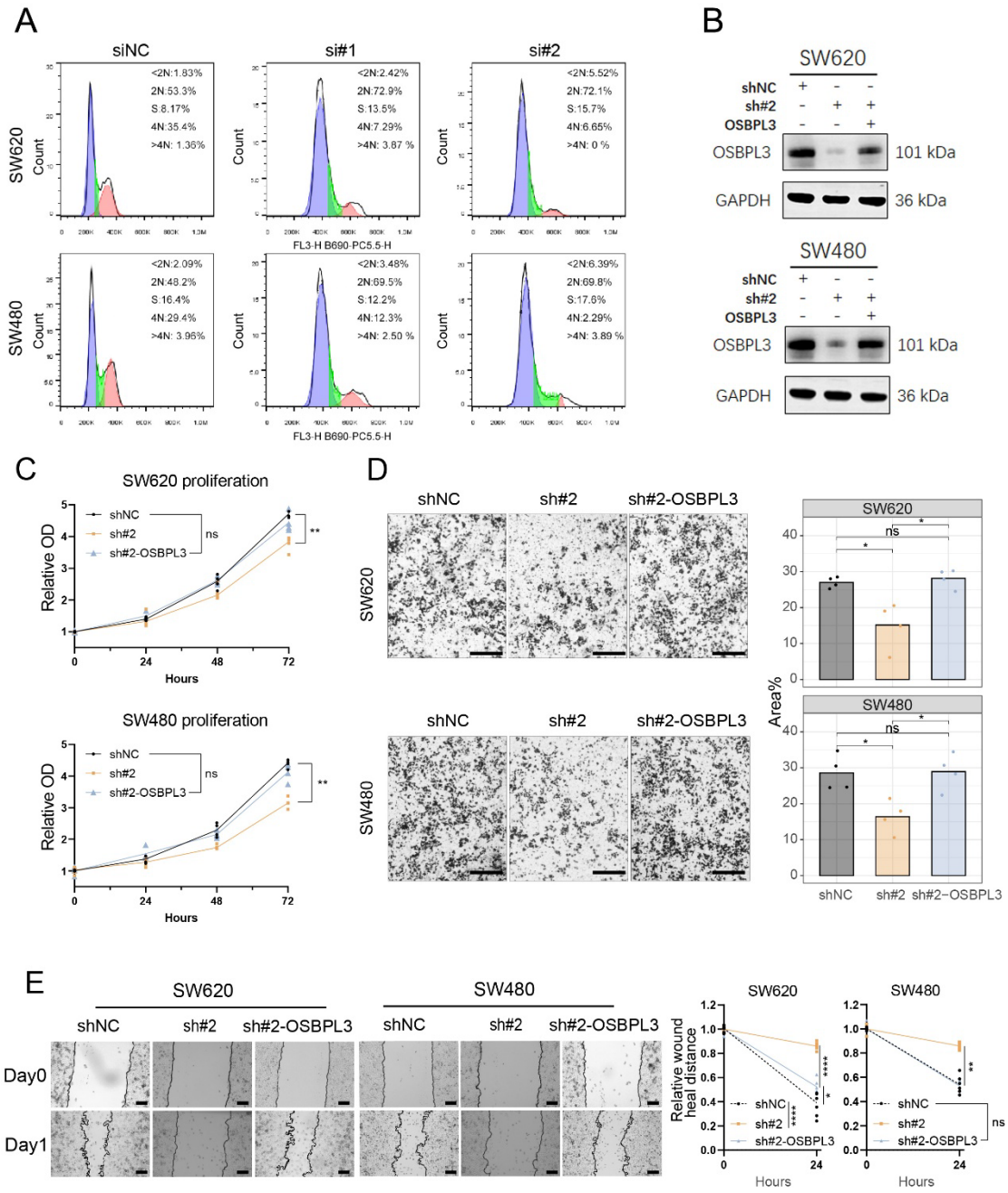

Supplementary Figure 1. Rescue of OSBPL3 knockdown phenotypes by re-expression of OSBPL3 in CRC cell lines. (A) Cell-cycle distribution after OSBPL3 knockdown in CRC cell lines; (B) Verification of OSBPL3 re-expression in stable knockdown cells. Immunoblotting of SW620 and SW480 cells expressing control shRNA (shNC), OSBPL3 shRNA (sh#2), or sh#2 plus OSBPL3 re-expression (sh#2-OSBPL3); (C) Proliferation assays (CCK-8 Cell Counting Kit, A311-01, Vazyme) with rescue. Growth curves (relative OD) for SW620 and SW480 cells with shNC, sh#2, or sh#2-OSBPL3 over 72 hours. (independent-samples t test used, **p < 0.01, n=4); (D) Transwell invasion with rescue. Representative micrographs and quantification for SW620 and SW480 cells with shNC, sh#2, or sh#2-OSBPL3. (independent-samples t test used, *p < 0.01, ns=not significant, n=4) (Scale bar = 100μm); (E) Wound-healing migration with rescue. Representative images at Day 0 and Day 1 for SW620 and SW480 cells with shNC, sh#2, or sh#2-OSBPL3, and corresponding quantification of relative wound closure

over 24 hours. (independent-samples t test used, *p < 0.05, **p<0.01, ****p<0.0001, ns=not significant, n=6) (Scale bar = 200μm).

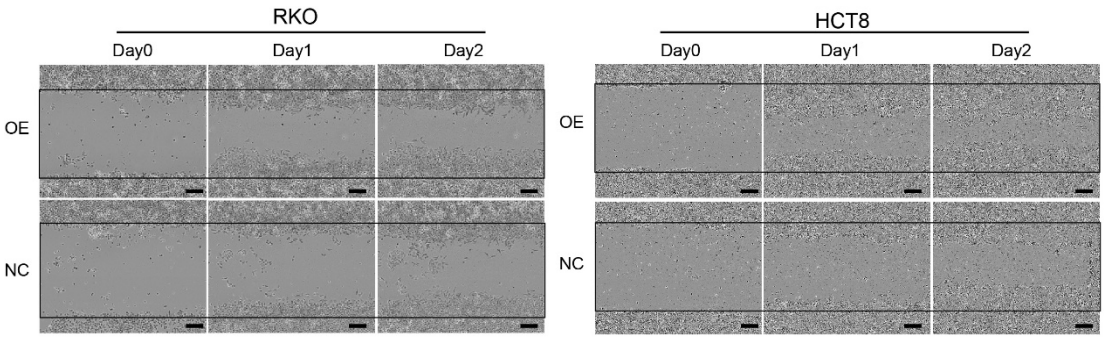

Supplementary Figure 2. Wound-healing assays following OSBPL3 overexpression. (Scale bar = 200μm).

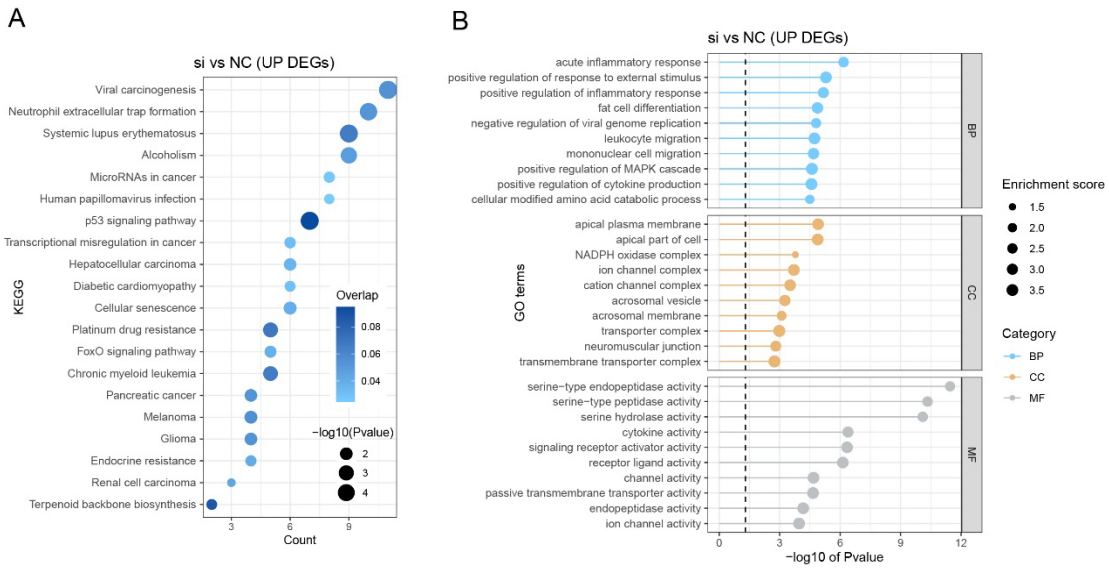

Supplementary Figure 3. Pathway and Gene Ontology enrichment of genes upregulated.

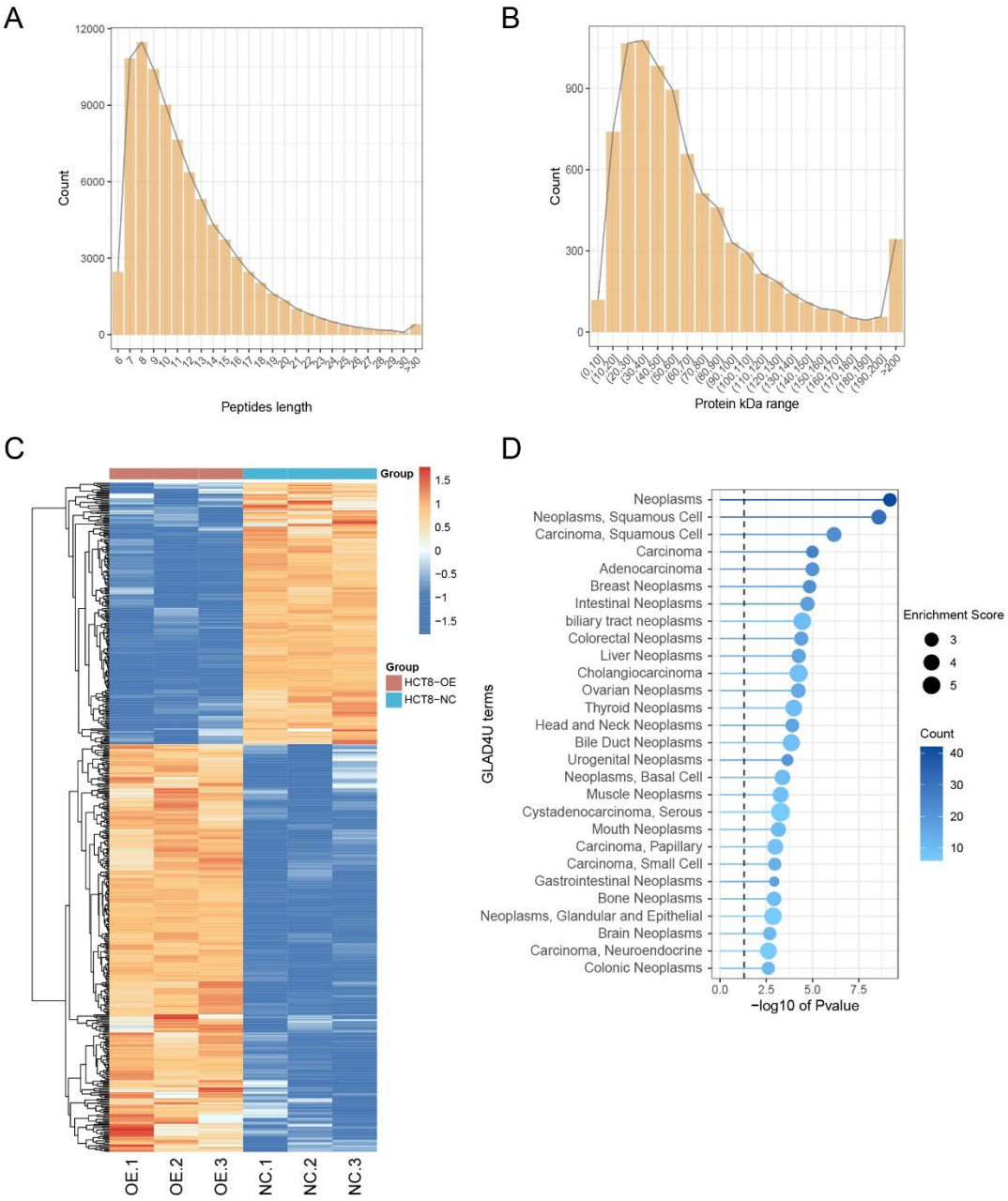

Supplementary Figure 4. TMT proteomics result. (A) Distribution plot of peptide lengths detected by protein mass spectrometry; (B) Distribution plot of protein molecular weights (kDa) identified through mass spectrometry; (C) Heatmap displaying differential protein expression between the overexpression and control groups at the protein level. (D) GALD4U pathway enrichment analysis of upregulated DEPs of OE group.

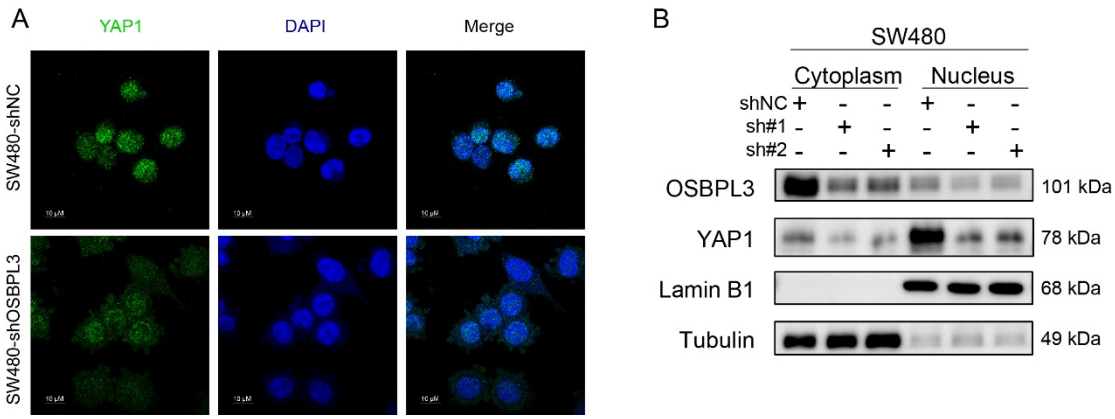

Supplementary Figure 5. IF result. (A) Subcellular localization changes of YAP1 in SW480 cells after OSBPL3 knockdown as observed by confocal microscopy; (B) Changes in protein levels of YAP1 and OSBPL3 in the nucleus and cytoplasm of SW480 cells following OSBPL3 knockdown.

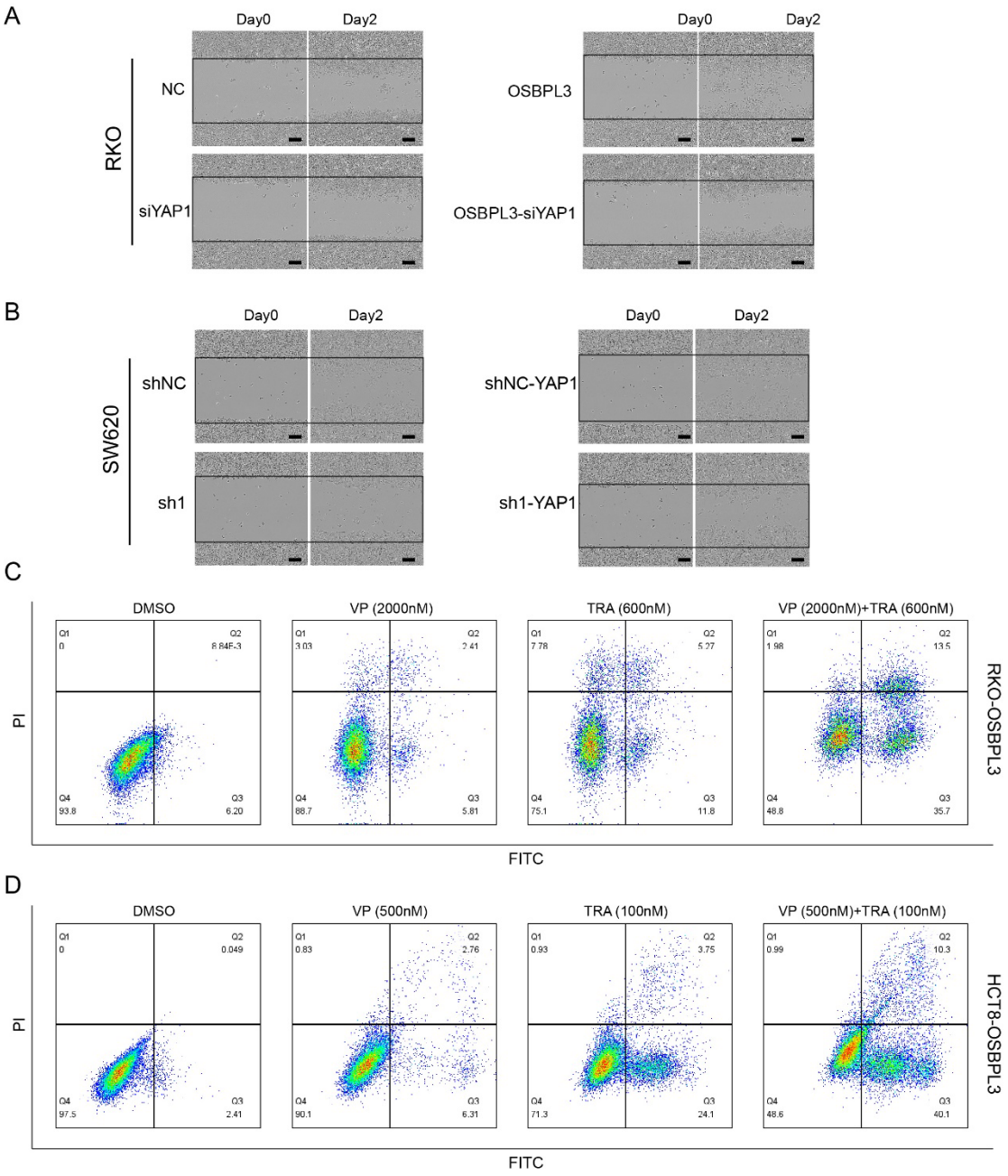

Supplementary Figure 6. Rescue results. (A) Scratch assay showing the impact of YAP1 knockdown on cell migration ability in RKO cells with OSBPL3 overexpression (Scale bar = 200μm). (B) Scratch assay showing the impact of YAP1 overexpression on cell migration ability in SW620 cells with OSBPL3 knockdown (Scale bar = 200μm). (C-D) Flow cytometric apoptosis analysis of OSBPL3-overexpressing RKO and HCT8 cells treated with VP and TRA, either alone or in combination. TRA, trametinib; VP, Verteporfin.

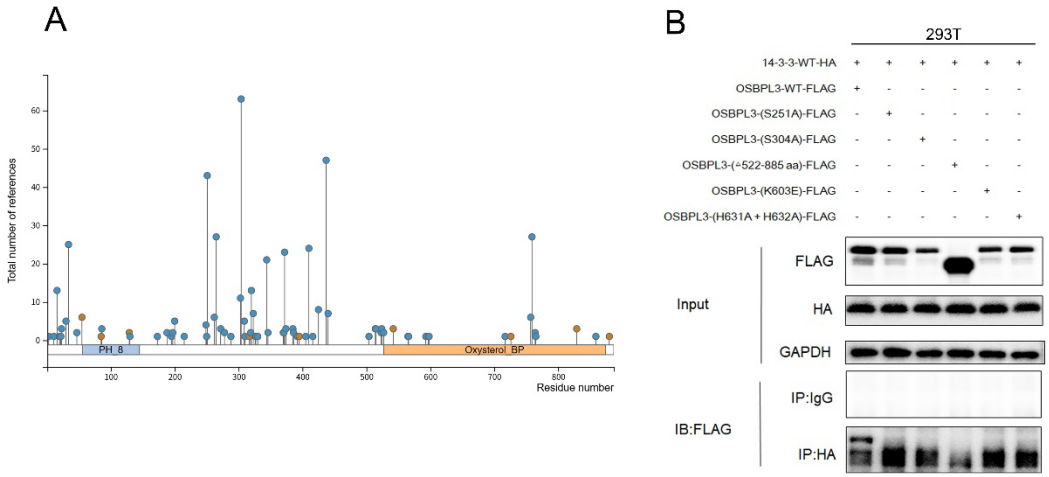

Supplementary Figure 7. OSBPL3 phosphorylation landscape and requirement of the C-terminus—but not single phosphosites or lipid binding—for 14-3-3 interaction.
(A) Distribution of reported phosphorylation sites across OSBPL3, compiled from PhosphoSitePlus.
(B) Co-immunoprecipitation of OSBPL3 variants with 14-3-3 in 293T cells.

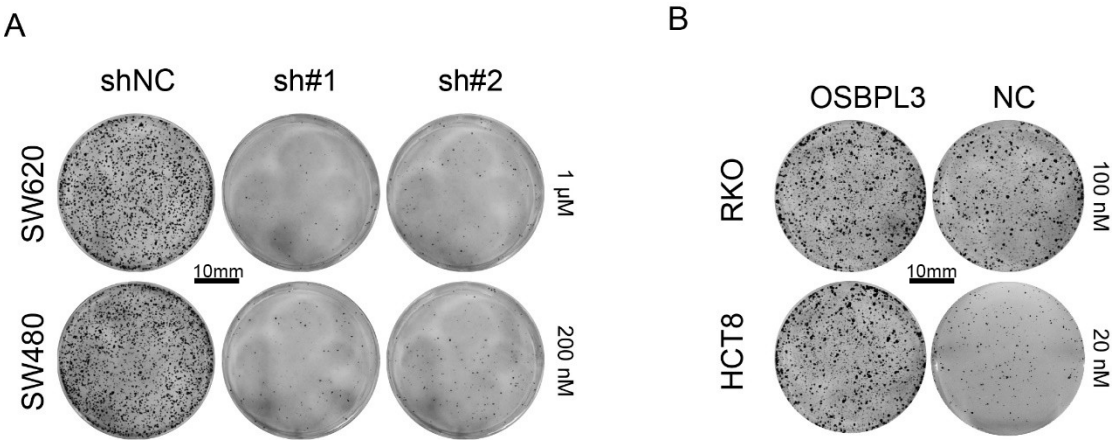

Supplementary Figure 8. Colony formation result. (A) Colony formation assay in SW620 and SW480 cells with OSBPL3 knockdown under the same concentration of TRA inhibition; (B) Colony formation assay in RKO and HCT8 cells overexpressing OSBPL3 under the same concentration of TRA inhibition. (Scale bar = 10mm)

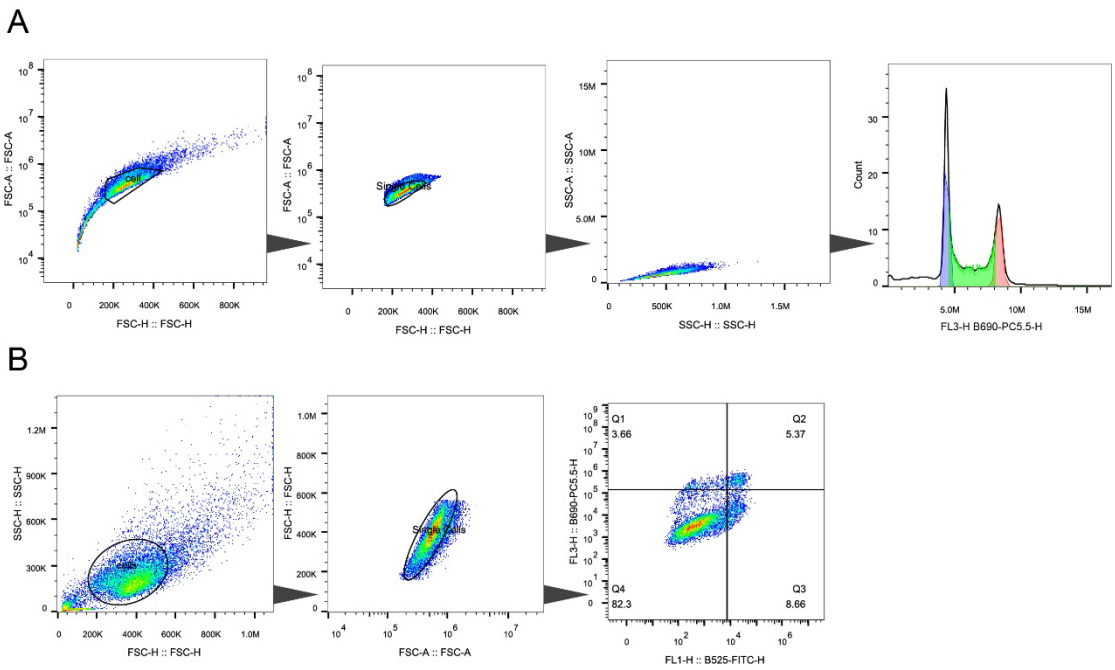

Supplementary Figure 9. Gating strategy for flow cytometric analysis. (A) Representative gating strategy for cell cycle analysis. Sequential plots show the identification of the cell population based on forward scatter (FSC) and side scatter (SSC), followed by doublet exclusion using FSC-A vs. FSC-H and SSC-A vs. SSC-H. The final histogram displays the DNA content distribution (FL3-H) used to determine cell cycle phases.
(B) Representative gating strategy for apoptosis analysis. Cells were first identified by light scatter properties (FSC-H vs. SSC-H), followed by doublet exclusion (FSC-A vs. FSC-H). The final dot plot shows the quadrant gating of Annexin V-FITC (FL1-H) versus PI (FL3-H) staining to distinguish viable (Q4), early apoptotic (Q3), late apoptotic (Q2), and necrotic cells (Q1). Arrows indicate the gated parent population displayed in the subsequent window.

Supplementary Table 1. Cell line background information.

Cell Line	Origin/Source	Patient Details	MSI Status	Key Mutations/Genetic Features
DLD-1	Colorectal adenocarcinoma, large intestine	Adult male, Dukes' type C	MSI	KRAS (G13D), PIK3CA (E545K; D549N), TP53 (S241F); POLD1 (R689W); CIMP+; pseudodiploid karyotype with dir dup(2)(p13-p23); high SNV load (592); oncogenes: myc+, myb+, ras+, fos+, sis+, p53+
HCT-116	Colorectal carcinoma, colon	48-year-old male, Dukes' type D	MSI	KRAS (G13D), PIK3CA (H1047R), TP53 (wild type); β-catenin (del codon 45); CIMP+; near-diploid karyotype with markers like t(9q;?16p-); CMS4; high SNV/indel count

HCT-8	Ileocecal colorectal adenocarcinoma, large intestine	67-year-old male	MSS	Limited specific mutations reported; tumorigenic; expresses CEA, alkaline phosphatase, keratin; higher CNA load (12–69%); CMS2; isoenzymes: AK-1 (1), GLO-I (2)
HT-29	Colorectal adenocarcinoma, primary tumor	44-year-old female, Dukes' type C	MSS	BRAF (V600E), PIK3CA (P449T), TP53 (R273H); CIMP+; hypertriploid karyotype (modal 71) with 17 markers; oncogenes: myc+, ras+, myb+, fos+, sis+, p53+; high CNA; colon-like, CMS2/3
LoVo	Colorectal adenocarcinoma, metastatic nodule (left supraclavicular)	56-year-old male, Dukes' type C, grade IV	MSI	KRAS (G13D; A14V), TP53 (wild type); CIMP-; hyperdiploid karyotype; oncogenes: c-myc+, K-ras+, H-ras+, N-ras+, myb+, sis+, fos+; undifferentiated, CMS1/4; mesenchymal morphology
RKO	Colon carcinoma, poorly differentiated	Not specified (adult)	MSI	BRAF (V600E), PIK3CA (H1047R), TP53 (wild type); CIMP+; high SNV/indel; PD-L1 expression; tumorigenic; lacks h-TRbeta1; undifferentiated, mesenchymal
SW-480	Colorectal adenocarcinoma, primary tumor	50-year-old male, Dukes' type B	MSS	KRAS (G12V), TP53 (R273H; P309S); CIMP-; hypotriploid karyotype with 11-12 markers; oncogenes: c-myc+, K-ras+, H-ras+, N-ras+, myb+, sis+, fos+; elevated p53; higher CNA
SW-620	Colorectal adenocarcinoma, lymph node metastasis	51-year-old male (same as SW-480), Dukes' type C	MSS	KRAS (G12V), TP53 (R273H; P309S); CIMP+ (partial); hyperdiploid karyotype (modal 50) with 11 markers; oncogenes: c-myc+, K-ras+, H-ras+, N-ras+, myb+, sis+, fos+; expresses CEA, TGF-alpha, matrilysin

Supplementary Table 2. List of Antibodies.

Antibody Name	Host /Clonality	Source	Catalog No.	Applications
OSBPL3	Rabbit Polyclonal	Abcam	ab192998	WB, IF, IP
OSBPL3	Rabbit Polyclonal	Sigma-Aldrich (Atlas Antibodies)	HPA000691	IHC
YAP1	Rabbit Monoclonal	Abcam	ab205270	WB, IF
p-YAP1 (Ser127)	Rabbit Monoclonal	Cell Signaling Technology (CST)	13008S	WB
p-YAP1 (Ser397)	Rabbit Monoclonal	Cell Signaling Technology (CST)	13619	WB

Supplementary Table 2. List of Antibodies.

Antibody Name	Host /Clonality	Source	Catalog No.	Applications
LATS1	Rabbit Monoclonal	Cell Signaling Technology (CST)	3477	WB
AREG	Rabbit Monoclonal	Cell Signaling Technology (CST)	13658	WB
CYR61	Rabbit Polyclonal	ABclonal	A1111	WB
Pan 14-3-3	Mouse Monoclonal	Santa Cruz Biotechnology	sc-133233	WB, IP
14-3-3 (Isoform specific)	Rabbit Polyclonal	Santa Cruz Biotechnology	sc-17287	IF, IP
GAPDH	Mouse Monoclonal	Abcam	ab8245	WB (Loading Control)
Tubulin	Mouse Monoclonal	Abcam	ab7291	WB (Loading Control)
FLAG Tag	Mouse Monoclonal	ABclonal	AE005	IP, WB
HA Tag	Rabbit Monoclonal	Cell Signaling Technology (CST)	3724S	IP, WB
HRP-conjugated Goat Anti-Rabbit IgG	Goat Polyclonal	ZSGB-BIO	ZB-2301	WB (Secondary)
HRP-conjugated Goat Anti-Mouse IgG	Goat Polyclonal	ZSGB-BIO	ZB-2305	WB (Secondary)

Figure 1E

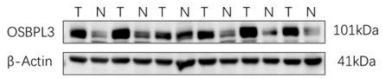

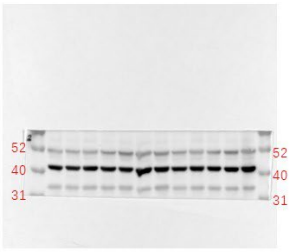

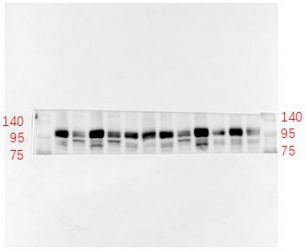

Figure 2A

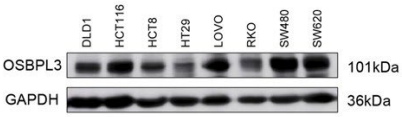

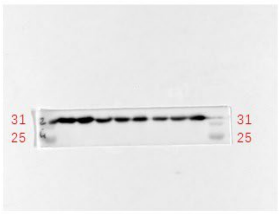

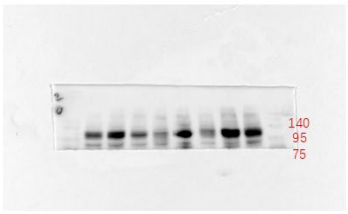

Figure 2E

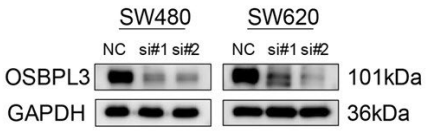

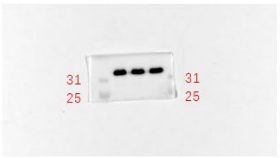

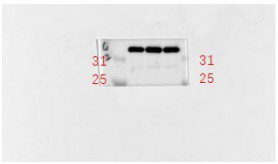

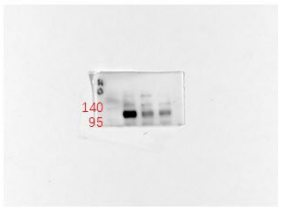

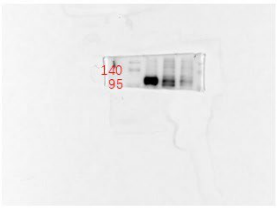

Figure 3A

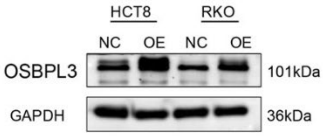

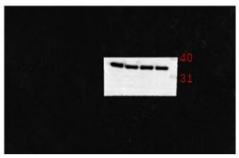

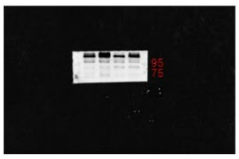

Figure 5A

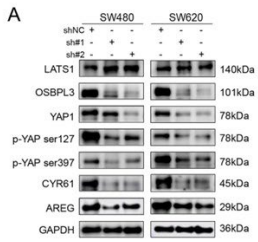

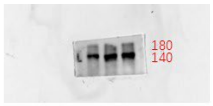

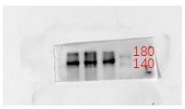

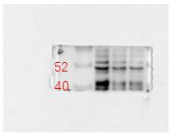

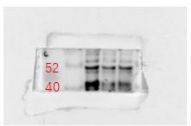

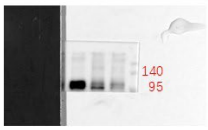

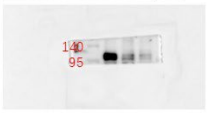

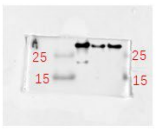

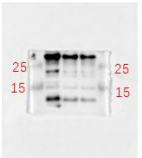

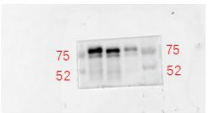

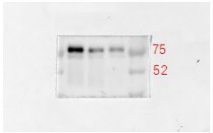

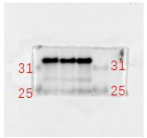

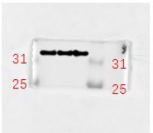

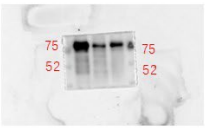

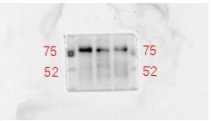

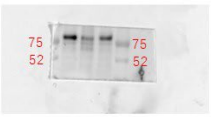

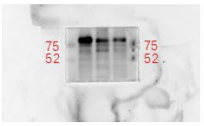

Figure 5B

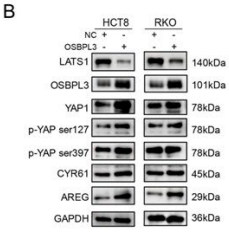

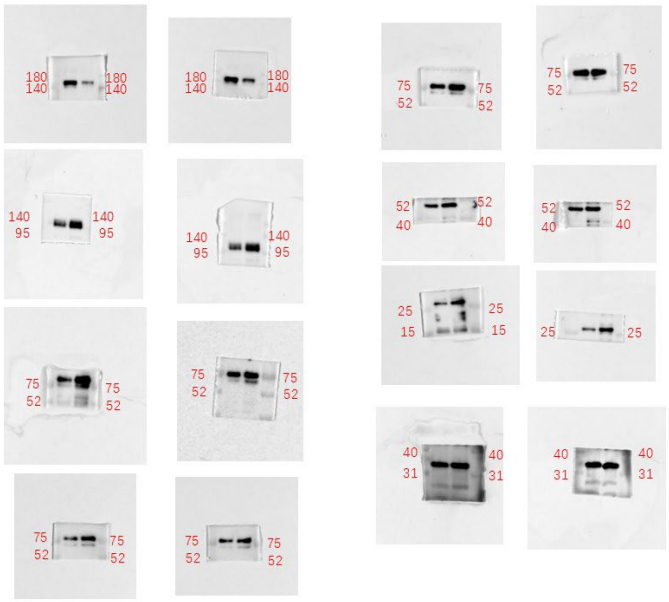

Figure 5D

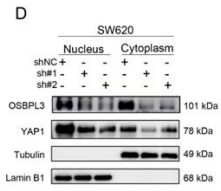

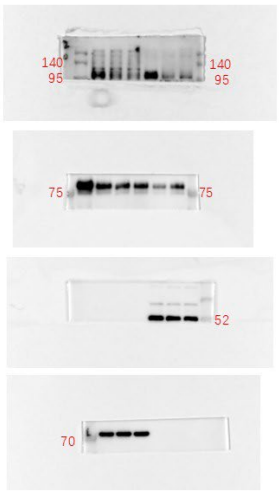

Figure 5E, 5H

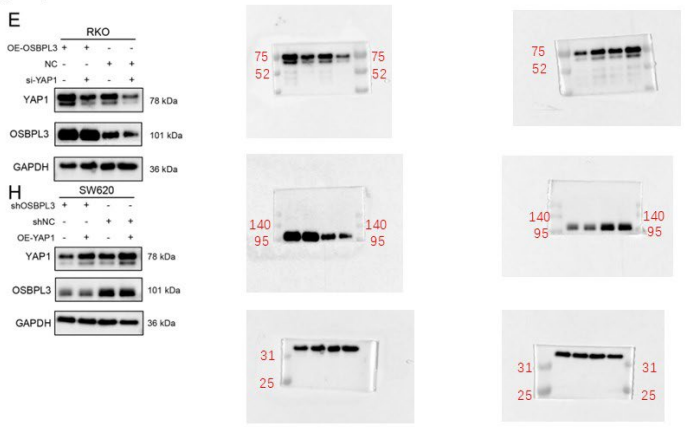

Figure 6C

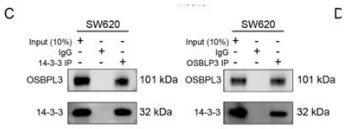

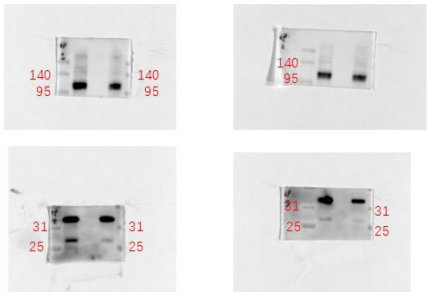

Figure 6H

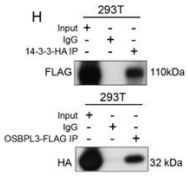

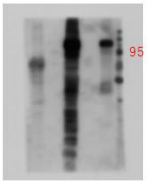

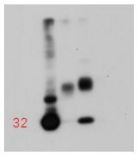

Figure 6I

I

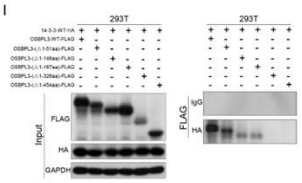

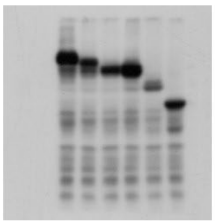

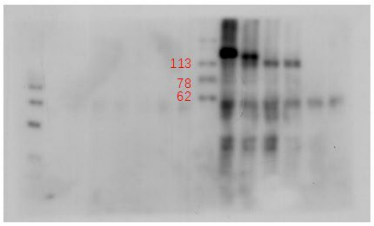

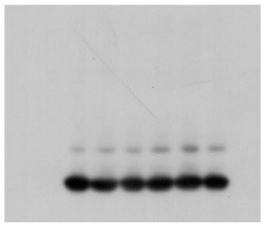

Figure 6J

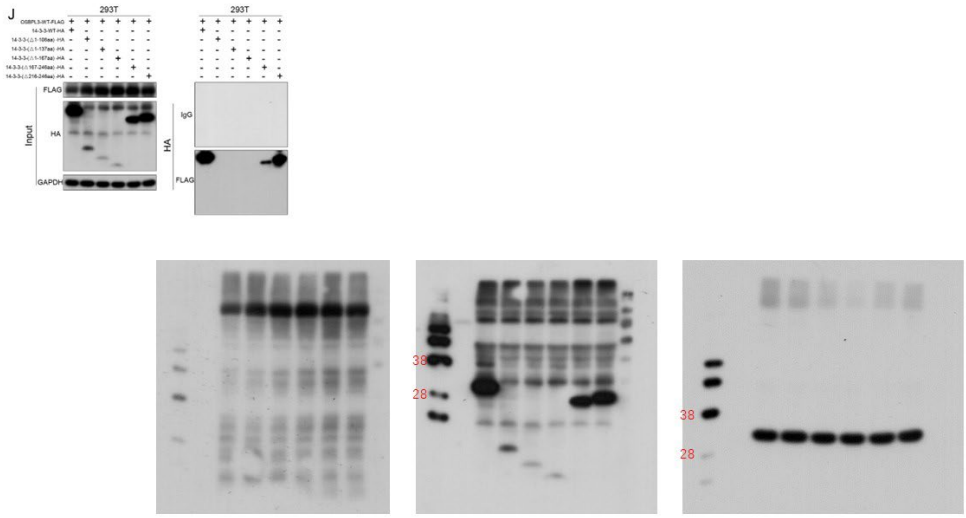

Supplementary Figure 1B

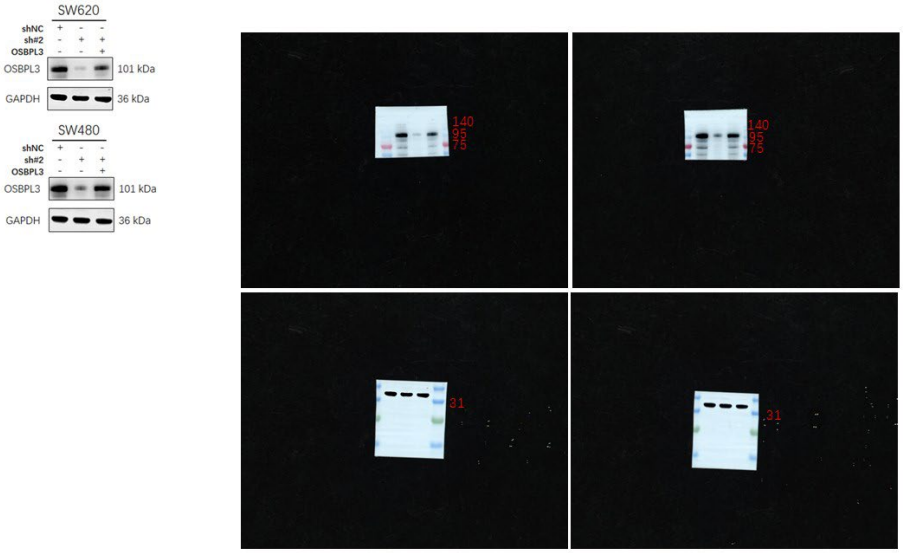

Supplementary Figure 5B

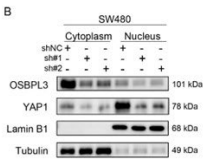

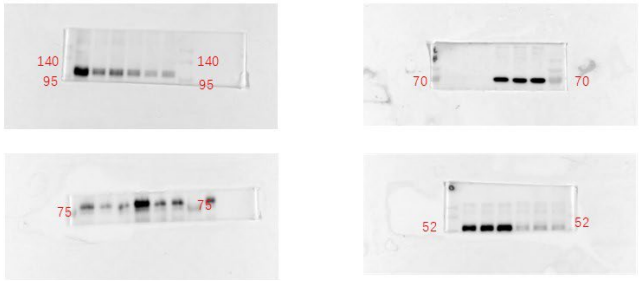

Supplementary Figure 8B